



This is a repository copy of *Dynamic behavior investigations and disturbance rejection predictive control of solvent-based post-combustion CO2 capture process*.

White Rose Research Online URL for this paper:  
<http://eprints.whiterose.ac.uk/141658/>

Version: Accepted Version

---

**Article:**

Wu, X., Shen, J., Li, Y. et al. (3 more authors) (2019) Dynamic behavior investigations and disturbance rejection predictive control of solvent-based post-combustion CO2 capture process. *Fuel*, 242. pp. 624-637. ISSN 0016-2361

<https://doi.org/10.1016/j.fuel.2019.01.075>

---

Article available under the terms of the CC-BY-NC-ND licence  
(<https://creativecommons.org/licenses/by-nc-nd/4.0/>).

**Reuse**

This article is distributed under the terms of the Creative Commons Attribution-NonCommercial-NoDerivs (CC BY-NC-ND) licence. This licence only allows you to download this work and share it with others as long as you credit the authors, but you can't change the article in any way or use it commercially. More information and the full terms of the licence here: <https://creativecommons.org/licenses/>

**Takedown**

If you consider content in White Rose Research Online to be in breach of UK law, please notify us by emailing [eprints@whiterose.ac.uk](mailto:eprints@whiterose.ac.uk) including the URL of the record and the reason for the withdrawal request.



[eprints@whiterose.ac.uk](mailto:eprints@whiterose.ac.uk)  
<https://eprints.whiterose.ac.uk/>

# Dynamic behavior investigations and disturbance rejection predictive control of solvent-based post-combustion CO<sub>2</sub> capture process

Xiao Wu<sup>a,\*</sup>, Jiong Shen<sup>a</sup>, Yiguo Li<sup>a</sup>, Meihong Wang<sup>b,\*</sup>,  
Adekola Lawal<sup>c</sup>, Kwang Y. Lee<sup>d</sup>

<sup>a</sup>Key laboratory of Energy Thermal Conversion and Control of Ministry of Education, Southeast University, Nanjing 210096, China

<sup>b</sup>Department of Chemical and Biological Engineering, The University of Sheffield, Sheffield S1 3JD, UK

<sup>c</sup>Process Systems Enterprise Ltd, 26-28 Hammersmith Grove, London W6 7HA, UK

<sup>d</sup>Department of Electrical and Computer Engineering, Baylor University, One Bear Place #97356, Waco, TX 76798-7356, USA

## Abstract

Increasing demand for flexible operation has posed significant challenges to the control system design of solvent-based post-combustion CO<sub>2</sub> capture (PCC) process: 1) the capture system itself has very slow dynamics; 2) in the case of wide range of operation, dynamic behavior of the PCC process will change significantly at different operating points; and 3) the frequent variation of upstream flue gas flowrate will bring in strong disturbances to the capture system. For these reasons, this paper provides a comprehensive study on the dynamic characteristics of the PCC process. The system dynamics under different CO<sub>2</sub> capture rates, re-boiler temperatures, and flue gas flow rates are analyzed and compared through step-response tests. Based on the in-depth understanding of the system behavior, a disturbance rejection predictive controller (DRPC) is proposed for the PCC process. The predictive controller can track the desired CO<sub>2</sub> capture rate quickly and smoothly in a wide operating range while tightly maintaining the re-boiler temperature around the optimal value. Active disturbance rejection approach is used in the predictive control design to improve the control property in the presence of dynamic variations or disturbances. The measured disturbances, such as the flue gas flow rate, is considered as an additional input in the predictive model development, so that accurate model prediction and timely control adjustment can be made once the disturbance is detected. For unmeasured disturbances, including model mismatches, plant behavior variations, etc., a disturbance observer is designed to estimate the value of disturbances. The estimated signal is then used as a compensation to the predictive control signal to remove the influence of disturbances. Simulations on a monoethanolamine (MEA) based PCC system developed on gCCS demonstrates the excellent effect of the proposed controller.

Keywords: Post-combustion carbon capture; Chemical absorption; Flexible operation; Dynamic behavior variations; Model predictive control; Disturbance rejection.

## 1. Introduction

Massive anthropogenic emissions of carbon dioxide is viewed as the main cause of global warming [1]. More than 30% of these emissions has the origin from fossil-fuel fired power plants, especially coal-fired power plants, which are the dominant devices in the power industry [2]. Therefore, CO<sub>2</sub> capture of coal-fired power plants is of great importance for mitigating global warming, greenhouse effect and related issues [3].

Many in-depth studies have been conducted for the carbon capture technology. Among them, chemical absorption based post-combustion CO<sub>2</sub> capture (PCC) is mature in technology and the installation of PCC devices requires only little modification to the existing power units. For these reasons, the PCC technology has been regarded as the most promising approach for the CO<sub>2</sub> removal of coal-fired power plants [3]. However, the high energy consumption required for solvent regeneration becomes barrier to its large-scale commercial deployment. To develop an efficient process for CO<sub>2</sub> separation from power plant flue gas, many studies on solvent selection [4-7], process configuration [8-10], parameter settings [6, 7] have been undertaken. These studies only focused on the steady-state optimization at a full operating condition.

In recent years, there has been an increasing demand on the flexible operation of PCC processes [11-20]. From external perspectives, with the extensive penetration of renewable energy in the power grid, the coal-fired power plants have to change their loading rapidly over a wide range to alleviate the impact of unstable renewable power supplies and varying load demand [21]. As a result, the flue gas flow rate will have significant variations. In this regard, the PCC plants are forced to operate in a flexible manner and follow these changes [12]. On the other hand, from internal perspectives, flexible operation is also a requirement for the PCC process itself, because flexible adjustment of CO<sub>2</sub> capture rate is the foundation for the entire power generation-carbon capture system to achieve a better scheduling considering the demands

\* Corresponding author.

E-mail address: wux@seu.edu.cn (X. Wu); Meihong.Wang@sheffield.ac.uk (M. Wang)

47 of power generation, energy consumption, system efficiency and carbon emission [12].

48 In this context, thorough understanding of the dynamic characteristics of the PCC system over the entire operating range  
49 and design of appropriate control system for the process have become emerging and concerned topics.

50 Establishing accurate dynamic PCC models and conducting experiments with the models is the most important step to  
51 understand system characteristics. Lawal et al. [22] investigated the dynamics of the standalone absorber based on dynamic  
52 modeling of the process. Their studies indicated that maintaining the ratio between lean solvent flow rate and flue gas flow  
53 rate is vital for partial load operation of the absorber. Their findings also showed that the CO<sub>2</sub> loading of lean solvent had  
54 significant impact on the performance of the absorber. Ziail et al. [23] developed a rate-based dynamic model for the CO<sub>2</sub>  
55 stripper system. Besides carrying out steady-state optimizations, the dynamic variation of steam rate and rich solvent rate,  
56 and their influence on the stripper performance were also investigated. In order to understand the dynamic behavior of the  
57 entire capture system, detailed analytical models composed by a series of mathematical equations are established based on  
58 a variety of simulation platforms, such as gPROMS [11], [12], Aspen Dynamics [15], [16], Modelica [24], [25], Matlab [26]  
59 and gCCS [27], [28]. The dynamic effects of solvent circulation rate, flue gas flow rate/composition and re-boiler heat duty  
60 on the key variables of the capture system were then studied through simulation on these models. In [29]-[31], data-driven  
61 identification models such as bootstrap aggregated neural network model [29], nonlinear autoregressive exogenous  
62 (NLARX) model [30] and neural fuzzy model [31] were developed for the solvent-based PCC system. Compared with the  
63 conventional first principle modeling approach, which needs a thorough understanding of the capture process and  
64 equipment design specifications, dynamic operation data is the only requirement for these models.

65 In [32] and [19], open-loop step response tests were carried out respectively at Esbjerg pilot plant and AGL Loy Yang  
66 power station to gain practical experience for the dynamic behavior of the PCC process. The parameters studied include  
67 flue gas flow rate, solvent flow rate and re-boiler duty. The experimental results showed the slow dynamics of the entire  
68 capture system and the strong couplings among multi-variables.

69 In Montañés et al. [25], dynamic model of a 600 MWe combined-cycle power plant with post-combustion CO<sub>2</sub>  
70 capture was developed using Modelica. The step response tests of the PCC system were then conducted at 100%, 80% and  
71 60% gas turbine load. The results showed that at lower gas turbine loading condition, the dynamics of PCC system was  
72 slower. In addition, they found that the plant responses corresponding to the increase or decrease of a certain variable were  
73 different.

74 The researches on the dynamic characteristics effectively provide directions for the control system design of the PCC  
75 process. Based on the results, a general control structure was proposed and used in [12], [15], [16], [33]-[37], which  
76 involved four key variables: the CO<sub>2</sub> capture rate, the re-boiler temperature, the lean solvent flow rate and the re-boiler  
77 heat duty. In most of these studies, 2-input 2-output decentralized proportional-integral (PI) control systems were designed,  
78 which used the lean solvent flow rate to adjust the CO<sub>2</sub> capture rate, and the re-boiler heat duty to adjust the re-boiler  
79 temperature. The simulations demonstrated that such a design could achieve a prompt control for the CO<sub>2</sub> capture rate and  
80 effectively alleviate the disturbances of the inlet flue gas flow rate and concentration variations. To maintain a better  
81 hydraulic stability of the absorber and stripper column, in Lin et al. [16], the lean solvent flow rate was fixed at a given  
82 value, and the re-boiler steam flow rate, which can change the lean solvent loading was selected to control the CO<sub>2</sub> capture  
83 rate.

84 Nittaya et al. [36] presented three decentralized PI control structures for the PCC process: 1) using the relative gain array  
85 (RGA) to pair the control loop; 2) heuristic approach using lean solvent flow rate to control the capture rate, and re-boiler  
86 heat duty to control the re-boiler temperature; and 3) heuristic approach using rich solvent flow rate to control the re-boiler  
87 temperature, and re-boiler heat duty to control the capture rate. Simulation results under different cases such as flue gas  
88 flow rate variation and set-point tracking showed that under normal working condition, the second control structure had the  
89 best performance. Authors then extended the pilot-scale PCC model to a commercial-scale model that matched a 750MWe  
90 coal-fired power plant using gPROMS [37]. The dynamic performance under the second control structure was evaluated  
91 through simulations. The results revealed that, the PCC plant was able to reject various disturbances and switch promptly  
92 between different operating points.

93 Panahi and Skogestad [33], [34] divided the operation range of PCC system into three regions according to the flue gas

94 flow rate of upstream power plant while considering the limitation of re-boiler heat duty. Steady-state optimizations were  
95 conducted for each region considering the energy consumption and penalty of CO<sub>2</sub> emission. The variables that were most  
96 closely related to the optimization performance were selected as controlled variables. Five control alternatives (four  
97 decentralized PI control structures and one multi-variable model predictive control structure) were then presented and the  
98 simulation results showed that the most advantageous PI control system was comparable to the predictive controller in the  
99 presence of large flue gas flow rate variation.

100 In order to better respond to the changes of flue gas flow rate, in [22] and [38], the idea of feed-forward control was  
101 applied to the PCC process control design. The solvent flow rate was required to vary synchronously with the flue gas flow  
102 rate (i.e., maintaining the L/G ratio) and the simulations demonstrated that such a design was more beneficial for attaining  
103 a designed CO<sub>2</sub> capture rate control.

104 Besides conventional PI controls, in recent years, a number of researchers have used the approach of model predictive  
105 control (MPC) for the capture process [13], [14], [17], [18], [35], [39]- [47]. The basic idea of MPC is to use an explicit  
106 process model to predict the future response of the plant and calculate the control inputs through the minimization of a  
107 dynamic objective function within the prediction horizon. Because of the MPC's natural advantages in handling  
108 multi-variable, slow dynamic, constrained system, better performance has been reported in the PCC controller design,  
109 compared to the PI control structures.

110 Due to the strong nonlinearity of the PCC system, [41] and [42] directly used the simplified nonlinear analytical model  
111 as the predictive model and designed nonlinear MPCs for the flexible operation of the PCC plant. The monoethanolamine  
112 (MEA) recirculation rate and re-boiler heat flow were considered as the manipulated variables. The simulation results on  
113 Modelica platform showed that the target CO<sub>2</sub> removal efficiency could be quickly tracked by the proposed nonlinear MPC  
114 in a wide operation range. Zhang et al. [43] identified a nonlinear additive autoregressive model with exogenous variables  
115 (NAARX model) as the predictive model, and developed a nonlinear MPC for the PCC process. Fast tracking performance  
116 can be achieved by the nonlinear MPC under wide changes in power load and CO<sub>2</sub> capture rate. However, the use of  
117 nonlinear MPC requires solving large-scale nonlinear dynamic optimization problems, which is time consuming and lacks  
118 computational robustness. To this end, linear MPCs have received more attention in the PCC controller design.

119 In Bedelbayev et al. [39], a linear MPC was developed for the absorber column control. The nonlinear first principle  
120 model of the absorber was linearized at given operating point and used as the predictive model. The lean solvent flow rate  
121 was selected as the manipulated variable to control the CO<sub>2</sub> capture rate. The inlet flue gas flow rate, temperature and CO<sub>2</sub>  
122 content were regarded as measured disturbances and used as a feed-forward signal to the MPC. Simulation results show  
123 that the linear MPC could attain a smooth capture rate tracking and quick response to the flue gas variation. Arce et al. [13]  
124 presented linear MPCs in a two-layer control structure for the independent solvent regeneration system. Steady-state  
125 economic optimization was performed in the high layer to provide optimal set-points. Two linear MPCs were developed in  
126 the low layer to track the desired re-boiler level, CO<sub>2</sub> capture molar flow and re-boiler pressure set-points. Zhang et al. [35]  
127 developed a linear MPC controller to adjust the CO<sub>2</sub> capture rate and re-boiler temperature for the integrated PCC process  
128 via MATLAB MPC toolbox. The lean solvent flow rate and re-boiler steam flow rate were selected as manipulated  
129 variables, and the flue gas flow rate, CO<sub>2</sub> composition, rich flow solvent flow rate were considered in the model  
130 development as disturbances. Different from the ordinary MPC which use a dynamic control objective function, in [18]  
131 and [44], the energy consumptions and CO<sub>2</sub> emissions were taken into account in the MPC's objective function. An optimal  
132 scheduling sequence was calculated for the PCC plant. In [40], [45], [46] different multi-variable linear MPCs were  
133 devised to regulate the core variables within the PCC process. Their results all indicated that using the MPC can achieve  
134 more superior performance for the flexible operation of the PCC system compared with the conventional PI controllers.

135 Despite the advantages of the MPC, the performance of MPC greatly relies on the quality of the predictive model. For  
136 the aforementioned linear MPCs, the predictive models were all developed through linearization of the mathematical  
137 model or through identification at a given operating point. Nevertheless, under the growing demand for flexible operation,  
138 the PCC system is required to face the varying flue gas and adjust its capture rate over a wide range. Meanwhile, the  
139 re-boiler temperature may also change during the unit load demand change. As these key variables deviate from the model  
140 design point, the dynamic behavior of the system will change greatly, and the resulting modeling mismatches will reduce

141 the quality of predictive control and, in severe cases, may destabilize the closed-loop control system.

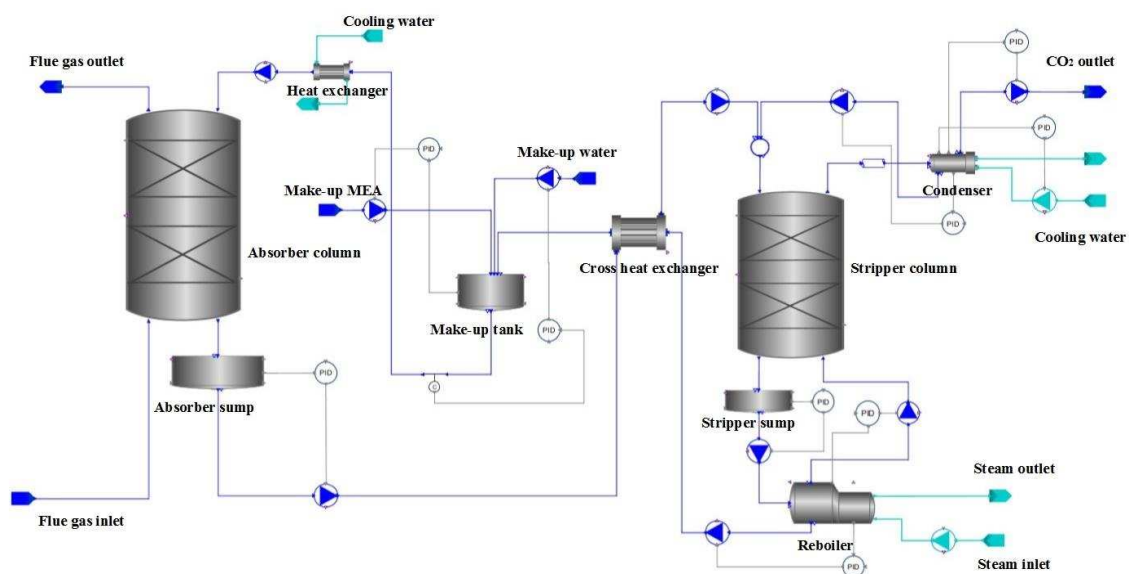
142 Owing to this difficulty, the existing linear MPCs only demonstrated their performance around the design point.  
143 Understanding the dynamic changes of the system and overcoming their impact on the control system is an important issue  
144 for the application of linear MPCs over a wide range of flexible operation of the PCC process.

145 To attain a wide range load change of the PCC process using the mature linear control technologies, in Wu et al. [47],  
146 three linear MPCs were preconfigured at 50%, 80% and 95% capture rate points. During operation, these three controllers  
147 were combined together based on the current capture rate to obtain the final global control output. Wu et al. [48] analyzed  
148 the dynamic behavior variation and nonlinearity distribution of the PCC process. Based on the results, a suitable operating  
149 region was selected, in which a simple linear MPC can achieve a satisfactory capture rate change control. However, the  
150 dynamic effect of flue gas flow rate on the PCC system and its variation under different operating conditions has not been  
151 analyzed. Moreover, how to effectively overcome the influence of dynamic variations or unknown disturbances was not  
152 studied in these works.

153 Given these observation, the first objective of this paper is to give new insight to the changes of PCC system dynamics  
154 under the variation of some key variables, such as flue gas flow rate, CO<sub>2</sub> capture rate and re-boiler temperature. Step  
155 response tests under different operating conditions are carried out to observe the changes of dynamics intuitively, and the  
156 corresponding response time constants and steady state gains are then analyzed. This investigation will provide useful  
157 guidance on the controller design, indicating how to avoid strong changes of PCC process dynamics during the control and  
158 provide possible applicable range of the linear MPC.

159 Then based on the investigation results, a disturbance rejection predictive controller (DRPC) is proposed for the flexible  
160 operation of the PCC process. A quasi-infinite horizon function is used as the objective function to improve the  
161 performance of conventional MPC and guarantee the stability of the closed-loop system. To overcome the dynamic  
162 behavior variations due to changes in operating point and the unknown disturbances due to equipment wear, a disturbance  
163 observer is devised to estimate and compensate for their impact on the set-point tracking. In order to enable the predictive  
164 controller to promptly adapt to the flue gas flow rate variation, the flue gas flow rate is considered as an additional input in  
165 the model development. Thus in the presence of flue gas flow rate change, correct prediction and control action can be  
166 provided on time. The simulation studies on an MEA-based post-combustion CO<sub>2</sub> plant developed on the gCCS platform  
167 validate the advantages and effectiveness of the proposed DRPC.

## 168 2. Process Description



169 Fig.1. Schematic diagram of solvent-based PCC process developed on the gCCS platform.

170 The solvent based post-combustion CO<sub>2</sub> capture system considered in this paper is matched with a small scale coal-fired  
171

power plant. 30 wt% MEA solvent, which is most commonly used in PCC process is selected as the CO<sub>2</sub> sorbent. At full load condition, the power plant can generate 0.13 kg/s flue gas (CO<sub>2</sub> concentration: 25.2 wt%) using the designated coal. After going through desulfurization, denitrification, dust removal and cooling processes, the flue gas is fed into the bottom of the packed-bed absorber column and contacts with the lean MEA solvent counter currently. The CO<sub>2</sub> in flue gas is absorbed chemically by the MEA solvent, yielding CO<sub>2</sub>-enriched solvent and the exited gas is vented into the atmosphere. Next, the rich solvent is pumped into the stripper column across a lean/rich heat exchanger, where it is heated by the steam drawn-off from the intermediate/low-pressure turbine crossover of power plant to release the CO<sub>2</sub>. The resulting lean solvent is then resent to the absorber and starts the next cycle. During heating, part of the water and MEA vapor is mixed with the removed CO<sub>2</sub>, thus a condenser is used to recollect the fugitive steam and MEA, the separated high purity CO<sub>2</sub> is then compressed and transported to storage.

The dynamic model of this PCC process is established using gCCS toolkit [27], [28], which can provide high-fidelity simulation for the CO<sub>2</sub> capture, transportation and storage. The specification and parameter selection for the major devices are based on the model developed in [12], which has been verified through field data. The process topology and nominal operation condition of the PCC model are displayed in Fig.1 and Tab.1.

Table 1. Nominal Operating Condition of Some Variables for the PCC Model Developed in gCCS

Variable	Unit	Value
Flue gas flow rate	[kg/s]	0.13
Flue gas CO <sub>2</sub> concentration	[wt%]	25.2
Flue gas absorber inlet temperature	[K]	313.15
Solvent flow rate	[kg/s]	0.5023
Lean solvent absorber inlet temperature	[K]	313.15
MEA concentration	[wt%]	30
Re-boiler pressure	[bar]	1.79
Re-boiler temperature	[K]	386
Re-boiler liquid level	[m]	0.25
Re-boiler steam flow rate	[kg/s]	0.0366
Condenser Pressure	[bar]	1.69
Condenser temperature	[K]	313.15
Absorber sump liquid level	[m]	1.25
Stripper sump liquid level	[m]	1.25
CO <sub>2</sub> capture rate	[%]	70

Within the PCC system, there are two variables that are of most concern in the controller design, the CO<sub>2</sub> capture rate and the re-boiler temperature. The CO<sub>2</sub> capture rate is defined as:

$$\text{CO}_2 \text{ Capture Rate} = \frac{\text{CO}_2 \text{ in the flue gas} - \text{CO}_2 \text{ in the clean gas}}{\text{CO}_2 \text{ in the flue gas}} \quad (1),$$

which reflects how well the capture plant completes the carbon reduction task. The re-boiler temperature determines the degree of solvent regeneration, which will affect the ability of lean solvent in CO<sub>2</sub> absorption. On the other hand, an excessively high temperature should be strictly avoided, because it will cause a severe MEA solvent degradation. Considering these issues, these two variables are selected as controlled variables in this study. The lean solvent and re-boiler steam flow rates are selected as the manipulated variables [12], [15], [16], [33]- [37], [41]- [43], [47].

The flexible operation requires the PCC plant to change its capture rate rapidly and follow the flue gas flow rate variation in a wide range. During the dynamic adjustment, the quick change of lean solvent and re-boiler steam flow rates may also cause significant variation of the re-boiler temperature. The change in operating condition of these key variables will cause the process dynamics change and bring in strong impact on the control system. Therefore, this paper investigates the dynamic behavior

change of the PCC system under the variation of CO<sub>2</sub> capture rate, flue gas flow rate and re-boiler temperature, providing guidance for the flexible operation of the PCC process and controller development. A disturbance rejection predictive controller is then designed to track the desired CO<sub>2</sub> capture rate in a wide range and maintain the re-boiler temperature at optimal point.

Besides the CO<sub>2</sub> capture rate and re-boiler temperature, there are many other variables need to be maintained to guarantee a safe operation of the PCC process. These variables are not strongly coupled or are easily controlled, therefore, PI controllers are designed to maintain them at given levels, which are shown in Fig. 1. Developing a centralized MPC control involving so many variables is a challenging task. Accurate predictive model is difficult to be identified and the receding-horizon calculation of the optimal control sequence is time consuming. Moreover, it is difficult to determine the sampling time of the centralized MPC, because the responses of the variables may be on different time scales.

### 3. Investigation of the dynamic behavior variation for the PCC process

In this section, step response tests under different working conditions are performed to give an intuitive analysis for the dynamic behavior variation of the solvent-based post-combustion CO<sub>2</sub> capture process. Different from the conventional 2×2 system analysis that only considers the dynamics between MVs (lean solvent and steam flow rates) and CVs (capture rate and re-boiler temperature), the influence of main disturbance: the flue gas flow rate has also been studied. Three groups of step response tests are conducted to analyze the dynamic behavior of PCC process under: i) different CO<sub>2</sub> capture rates; ii) different flue gas flow rates; and iii) different re-boiler temperatures.

In all the step response tests, the CO<sub>2</sub> capture rate and re-boiler temperature controllers are placed in an open-loop state, while other variables are kept controlled to ensure a normal operating of the CO<sub>2</sub> capture process. Step signals in magnitude of +5% of the respective steady-state values are added to the lean solvent, re-boiler steam and flue gas flow rate channels respectively at different operating points. The relative variation of capture rate and re-boiler temperature based on their initial steady-state values are then calculated and shown in Figs. 2-4.

#### 3.1. CO<sub>2</sub> capture rate change

To investigate the dynamic behavior variation of the PCC process under different CO<sub>2</sub> capture rates, step response tests are carried out at 50%, 60%, 70%, 80%, 90% and 95% capture rates. For all simulation tests in this group, the flue gas flow rate is maintained at 0.13kg/s and the re-boiler temperature is set as 386K initially to avoid their influence.

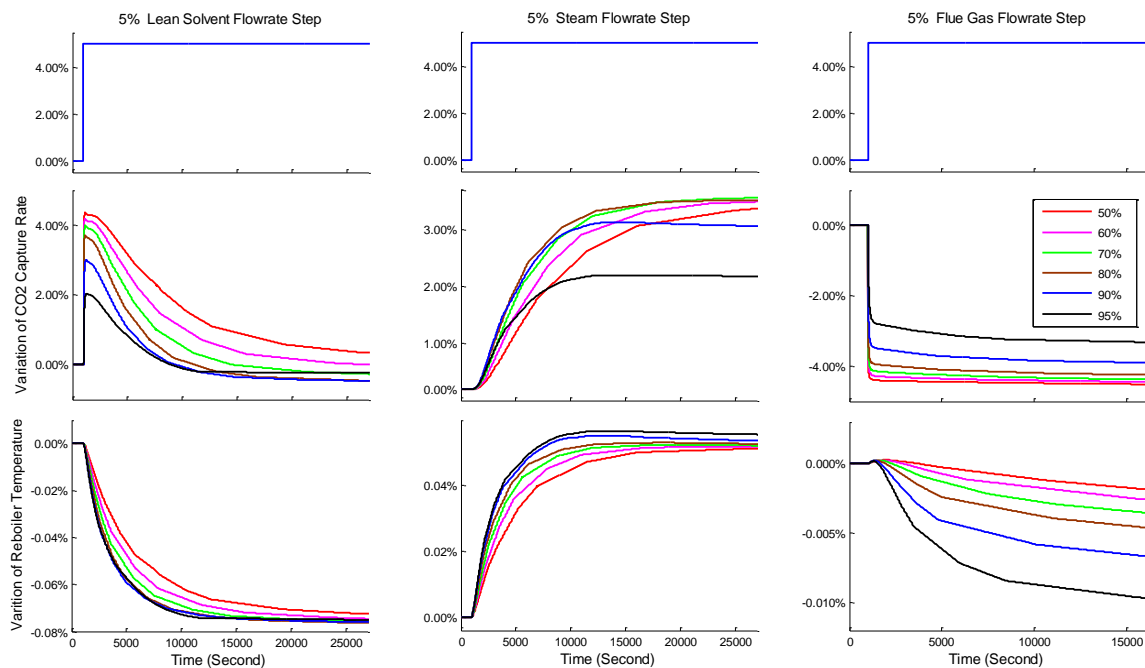


Fig. 2. Responses of the PCC process at six different CO<sub>2</sub> capture rates corresponding to 5% lean solvent flow rate step input (left column), 5% steam flow rate step input (middle column) and 5% flue gas flow rate step input (right column).

At  $t=1000s$ , step signals in magnitude of +5% of the steady-state values are added to the lean solvent flow rate, re-boiler steam flow rate and flue gas flow rate channels respectively at different CO<sub>2</sub> capture rates. The left column of Fig. 2 shows the step responses of the PCC system corresponding to the step inputs of lean solvent flow rate. At the beginning of the step test, since more lean solvent is fed into the absorber column, more CO<sub>2</sub> in the flue gas can be absorbed, resulting in a prompt rise of CO<sub>2</sub> capture rate. However, as the re-boiler steam flow rate remains at the same level while the rich solvent enters the re-boiler is increased, the re-boiler temperature gradually drops. As a result, less CO<sub>2</sub> can be removed from the solvent and the loading of the lean solvent fed back to the absorber will rise. Therefore, the CO<sub>2</sub> capture rate will drop back to the previous level after a while and its response speed is slower than that of the re-boiler temperature. It takes more than 10,000 seconds for the PCC process to enter the new steady state, which fully illustrates the system's characteristics of large inertia. However, at the beginning of the step, the rapid impact of lean solvent flow rate on the CO<sub>2</sub> capture rate provides a useful way to achieve a flexible operation of the PCC system, even though it is temporary. On the other hand, the non-minimum phase behavior of the lean solvent flow rate-CO<sub>2</sub> capture rate loop will also bring in difficulties for the conventional feedback controller design.

The dynamic behavior change of the capture system under different capture rates can also be viewed in this column. Regarding the CO<sub>2</sub> capture rate channel, the overall trends of the responses are similar. However, as the capture rate increases, it becomes more difficult to capture the remaining CO<sub>2</sub> in the flue gas, the peak value of the step response drops, especially within 90%-95% capture rate region. On the other hand, the steady-state gains of the step responses slightly decrease and the response speed rises as the capture rate increases. Regarding the re-boiler temperature channel, the dynamic variation of the process is not strong, mainly reflected in the response speed, which has a slight increase as the capture rates rises.

The middle column of Fig. 2 shows the responses of the PCC process at different CO<sub>2</sub> capture rates corresponding to 5% steam flow rate step. The increase of re-boiler steam flow rate will increase the re-boiler temperature directly, as a result, more CO<sub>2</sub> will be released from the rich solvent. The decrease of CO<sub>2</sub> loading will then enhance the CO<sub>2</sub> absorption ability of the lean solvent, thus the CO<sub>2</sub> capture rate will be increased eventually. The response of re-boiler temperature is faster than the response of CO<sub>2</sub> capture rate, but overall very slow. The whole dynamic process will last for more than 10000s until the capture rate and re-boiler temperature enter the new steady-state. This slow dynamic brings challenges for the flexible operation of the PCC system.

The dynamic behavior change of the capture system under different capture rates is illustrated clearly in this column. Regarding the CO<sub>2</sub> capture rate channel, in the range of 50% to 80%, as the capture rate increases, the steady-state gains of the step responses are similar but the response speed slightly increases. When the capture rate rises to 90%, as most of the CO<sub>2</sub> in the flue gas has been gradually captured, the difficulty for the solvent to absorb the remaining CO<sub>2</sub> begins to increase. As a result, the steady state gain at 90% capture rate has dropped compared with the conditions of lower capture rates. Similarly, when the capture rate rises to 95%, it becomes much difficult to absorb the remaining CO<sub>2</sub> from the flue gas. A huge decrease in steady state gain can thus be found from the middle figure of this column. In terms of the re-boiler temperature, in the range of 50% to 95%, the steady-state gains of the step responses are similar and the response speed slightly increases as the capture rate increases.

We than show the responses of the PCC process corresponding to 5% flue gas flow rate step in the right column of Fig. 2. Because the lean solvent and steam flow rates within the PCC process are not changed, when the inlet flue gas flow rate increases, only a small part of the increased CO<sub>2</sub> can be captured in the absorber. Therefore, according to the calculation formula of capture rate (1), a significant decrease of CO<sub>2</sub> capture rate can be viewed within 100 seconds of the step test. On the other hand, since more CO<sub>2</sub> is absorbed, the rich solvent loading is increased, which will slightly decrease the re-boiler temperature and then continue decrease the CO<sub>2</sub> capture rate. However, these influence is very limited and can thus be ignored.

It can also be found that under different capture rates, the decrease level of capture rate is different: at high capture rate, capture the CO<sub>2</sub> in the increased flue gas is much easier than capture the remaining CO<sub>2</sub> in the original flue gas. Thus, under 95% and 90% capture rates, there are only 3.3% and 3.9% of capture rates drop corresponding to a 5% flue gas flow rate increase, while around 4.3% of the capture rate drops have occurred under other cases.

The step response tests show that, within 50%-90% capture rate range, the dynamics of the PCC system are similar, nevertheless, its dynamic behavior at 95% capture rate is much different, which is prominently reflected in the re-boiler steam-

capture rate channel. Some typical features of the lean solvent flow rate and re-boiler steam flow rate step responses are shown in Tabs. 2 and 3. For the flue gas flow rate step, since its dynamic response is relatively simple, the main parameters are not listed in the table.

Table 2. Typical features for the responses of the PCC process at different CO<sub>2</sub> capture rates corresponding to 5% lean solvent flow rate step input.

CO <sub>2</sub> Capture Rate	Response of CO <sub>2</sub> Capture Rate			Response of Re-boiler Temperature		
	Steady State Gain	Peak Time	Transient Time	Steady State Gain	Maximum Speed Time*	Transient Time*
50%	0.305%	1169s	19800s	-0.073%	1680s	15962s
60%	0.003%	1173s	17898s	-0.075%	1680s	13592s
70%	-0.265%	1195s	15268s	-0.076%	1620s	11878s
80%	-0.362%	1197s	13633s	-0.071%	1560s	10754s
90%	-0.459%	1234s	12267s	-0.076%	1380s	9868s
95%	-0.226%	1330s	9104s	-0.075%	1380s	8075s

\* Maximum speed refers to the maximum average rate of change within 60 seconds of the step response;

Transient time refers to the time it takes for the step response curve to enter the last 5% of the total change (and no longer goes out).

Table 3. Typical features for the responses of the PCC process at different CO<sub>2</sub> capture rates corresponding to 5% steam flow rate step input.

CO <sub>2</sub> Capture Rate	Response of CO <sub>2</sub> Capture Rate			Response of Re-boiler Temperature		
	Steady State Gain	Maximum Speed Time	Transient Time	Steady State Gain	Maximum Speed Time	Transient Time
50%	3.178%	3600s	21113s	0.051%	1680	13673s
60%	3.294%	3140s	17349s	0.052%	1620s	10824s
70%	3.358%	2640s	15700s	0.052%	1560s	9514s
80%	3.317%	2580s	11821s	0.053%	1440s	7565s
90%	2.864%	2160s	9346s	0.054%	1440s	7218s
95%	1.982%	2400s	9233s	0.056%	1440s	7565s

### 3.2. Flue gas flow rate change

To investigate the dynamic behavior variation of the PCC process under different flue gas flow rates, step response tests are carried out under 0.07kg/s, 0.10 kg/s, 0.13 kg/s and 0.15 kg/s flue gas flow rates. For all simulation tests in this group, the CO<sub>2</sub> capture rate and the re-boiler temperature are set at 80%, 386K point initially to avoid their influence. The step responses of the PCC system corresponding to the lean solvent flow rate, re-boiler steam flow rate and flue gas flow rate step inputs are shown in Fig. 3.

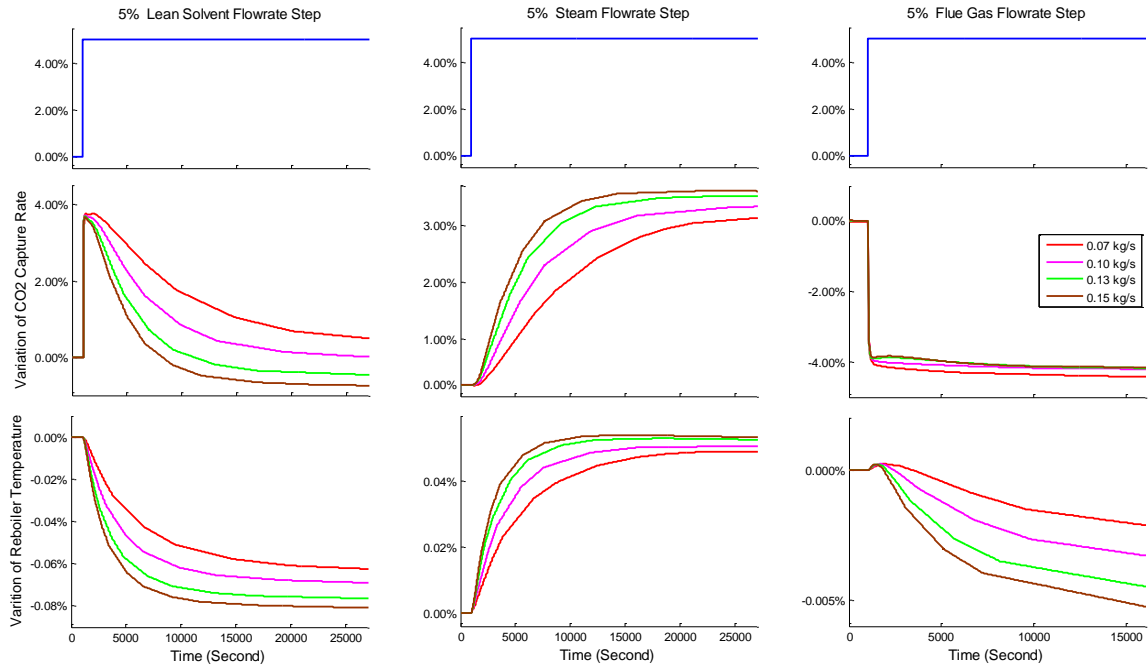


Fig. 3. Responses of the PCC process at four different flue gas flow rates corresponding to 5% lean solvent flow rate step input (left column), 5% steam flow rate step input (middle column) and 5% flue gas flow rate step input (right column).

As shown in Fig. 3, there are also some differences for the PCC system dynamics under different flue gas flow rates. Regarding the lean solvent flow rate step (left column), for both the capture rate and re-boiler temperature channels, as the flue gas flow rate rises, the steady-state gain of the step response decreases and the rate of the response increases. Similarly, in case of re-boiler steam flow rate step (middle column), for both the capture rate and re-boiler temperature channels, the steady-state gain and rate of the response increase as the flue gas flow rate rises. However, these dynamic variations are quite limited. There are no major differences for the main trends of the step responses under different flue gas flow rates. In addition, the investigation results also reflect that the PCC system is easily controlled at higher loads, because the manipulated variables can regulate the controlled variables more quickly. For the flue gas flow rate step (right column), the dynamic variation of the PCC system under different flue gas flow rate is very small and can be ignored. Some typical features of the lean solvent flow rate and re-boiler steam flow rate step responses are shown in Tabs. 4 and 5.

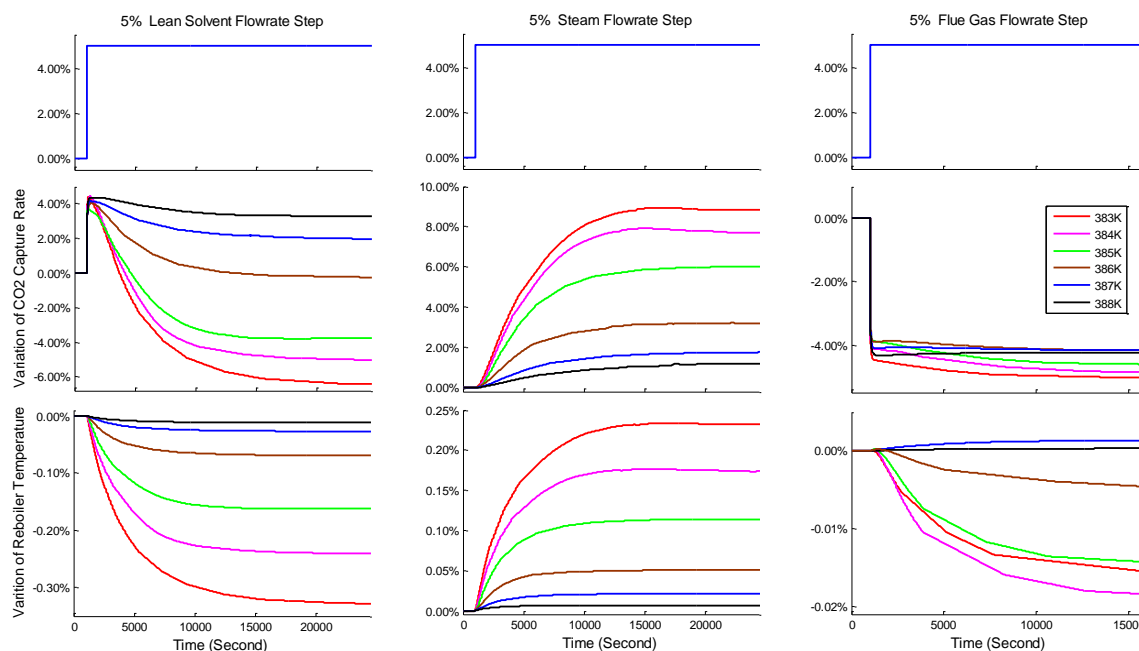
Table 4. Typical features for the responses of the PCC process at different flue gas flow rates corresponding to 5% lean solvent flow rate step input.

Flue Gas Flow Rate	Response of CO <sub>2</sub> Capture Rate			Response of Re-boiler Temperature		
	Steady State Gain	Peak Time	Transient Time	Steady State Gain	Maximum Speed Time	Transient Time
0.07kg/s	0.471%	2003s	21106s	-0.063%	1860s	16786s
0.10kg/s	0.009%	1202s	17252s	-0.069%	1620s	12683s
0.13kg/s	-0.362%	1197s	13633s	-0.071%	1560s	10754s
0.15kg/s	-0.745%	1184s	12270	-0.081%	1500s	9467s

Table 5. Typical features for the responses of the PCC process at different flue gas flow rates corresponding to 5% steam flow rate step input.

Flue Gas Flow Rate	Response of CO <sub>2</sub> Capture Rate			Response of Re-boiler Temperature		
	Steady State Gain	Maximum Speed Time	Transient Time	Steady State Gain	Maximum Speed Time	Transient Time
0.07kg/s	2.928%	4920s	19047s	0.049%	1680s	14255s
0.10kg/s	3.131%	2700	15602s	0.051%	1680s	10223s
0.13kg/s	3.317%	2580s	11821s	0.053%	1440s	7515s
0.15kg/s	3.404%	2220s	10149s	0.053%	1440s	6097s

309 To investigate the dynamic behavior variation of the PCC process under different re-boiler temperatures, step response tests  
 310 are carried out under 383K, 384K, 385K, 386K, 387K and 388K re-boiler temperatures. For all simulation tests in this group, the  
 311 flue gas flow rate is maintained at 0.13kg/s and the CO<sub>2</sub> capture rate is set as 80% initially to avoid their influence. The step  
 312 responses of the PCC system corresponding to the lean solvent flow rate step input are shown in Fig. 4. It can be seen clearly that,  
 313 under different re-boiler temperatures, the steady state gains, response speeds and even the variation trends of the step responses  
 314 are quite different.



315  
 316 Fig. 4. Responses of the PCC process at six different re-boiler temperature corresponding to lean solvent flow rate step input.

317 In the low temperature range of 383K to 385K, the re-boiler heat duty is relatively insufficient, part of the CO<sub>2</sub> cannot be  
 318 stripped from the rich solvent. Under this condition, the increase of lean solvent flow rate (left column) will make the re-boiler  
 319 temperature drop more and increase the CO<sub>2</sub> loading of the lean solvent. As a result, the CO<sub>2</sub> capture rate will decline to a lower  
 320 level eventually. In the high temperature range of 387K to 388K, surplus of re-boiler heat duty has occurred. In this case, the  
 321 increase of lean solvent flow rate will only cause a slight drop of the re-boiler temperature and increase the CO<sub>2</sub> loading of the  
 322 lean solvent a little bit. Therefore, the CO<sub>2</sub> capture rate will stay at a higher level eventually. Between these two situations, 386K  
 323 is the optimal re-boiler temperature, and under this temperature, the increase of lean solvent flow rate and the resulting increase  
 324 of lean solvent loading will make the CO<sub>2</sub> capture rate finally go back to the previous level.

325 As shown in the middle column, under lower re-boiler temperature, the increase of steam flow rate will cause more increase in  
 326 the capture rate and re-boiler temperature. The reason is that, under lower re-boiler temperature, the heat duty is relatively  
 327 insufficient, thus the increase of steam flow rate is easier to make the re-boiler temperature rise more, which will achieve a better  
 328 reduction in lean solvent loading and enhance the CO<sub>2</sub> capture rate. A significant difference of steady-state gains can be viewed  
 329 within 385K-387K region for both the CO<sub>2</sub> capture rate and re-boiler temperature channels.

330 Similarly, for the flue gas flow rate steps (right column), in case of excess re-boiler heat duty (387K-388K), the flue gas flow rate  
 331 rate increase has little effect on the re-boiler temperature. However, when the re-boiler heat duty is insufficient (383K-386K), the  
 332 flue gas flow rate increase will make the re-boiler temperature drop more and further cause more drops in CO<sub>2</sub> capture rate.

333 The investigation results show that the dynamic behavior of the PCC systems changes significantly as the re-boiler  
 334 temperature change, especially around 386K, which is the optimal re-boiler temperature for the system operation. This finding  
 335 also reminds us, it is of great importance to maintain the re-boiler temperature closely around the given optimal set-point, so that  
 336 the adverse effects of strong dynamic behavior variation on the operation control of PCC process can be alleviated.

337 Some typical features of the lean solvent flow rate and re-boiler steam flow rate step responses are shown in Tabs. 6 and 7.

Table 6. Typical features for the responses of the PCC process at different re-boiler temperatures corresponding to 5% lean solvent flow rate step input.

Re-boiler Temperature	Response of CO <sub>2</sub> Capture Rate			Response of Re-boiler Temperature		
	Steady State Gain	Peak Time	Transient Time	Steady State Gain	Maximum Speed Time	Transient Time
383K	-6.421%	1153s	12781s	-0.329%	1440s	11483s
384K	-5.025%	1319s	11749s	-0.241%	1440s	10035s
385K	-3.733%	1088s	9807s	-0.162%	1560s	8306s
386K	-0.362%	1197s	13633s	-0.071%	1560s	10754s
387K	1.973%	1313s	15470s	-0.028%	1380s	12271s
388K	3.265%	1633s	15277s	-0.012%	1260s	9570s

Table 7. Typical features for the responses of the PCC process at different re-boiler temperatures corresponding to 5% steam flow rate step input.

Re-boiler Temperature	Response of CO <sub>2</sub> Capture Rate			Response of Re-boiler Temperature		
	Steady State Gain	Maximum Speed Time	Transient Time	Steady State Gain	Maximum Speed Time	Transient Time
383K	8.838%	2060s	10359s	0.232%	1340s	9171s
384K	7.704%	2300s	9313s	0.174%	1400s	7993s
385K	6.021%	2480s	12068s	1.142%	1520s	8812s
386K	3.317%	2580s	11821s	0.053%	1440s	7515s
387K	1.757%	3080s	14425s	0.022%	1040s	8939s
388K	1.200%	17300s	16270s	0.007%	1040s	3712s

According to the investigation results, the following conclusions can be made for the PCC system dynamics:

(1) In general, the dynamic response of PCC system is very slow, for both the lean solvent and re-boiler steam flow rate steps, more than 2 hours is needed for the system to reach the new steady-state. Meanwhile, there are strong couplings among multiple manipulated and controlled variables. These features bring in difficulties for achieving the flexible operation of PCC system;

(2) The lean solvent flow rate can change the CO<sub>2</sub> capture rate in 2-3 minutes at the beginning stage. Although this quick impact is only temporary, it will provide great help for improving the flexibility of the PCC system. This is the reason why good results can be achieved by using the lean solvent flow rate to control the CO<sub>2</sub> capture rate;

(3) The change of flue gas flow rate will influence the capture rate in a very quick manner, its influence on the re-boiler temperature is trivial;

(4) Under higher flue gas flow rate and capture rates (less than 90%) the PCC system responds more quickly and thus is easy to control;

(5) The dynamic behavior variation of PCC system is small for a CO<sub>2</sub> capture rate change within 50-90% range, however, when the capture rate rises to 95%, the dynamic behavior becomes quite different;

(6) The change of flue gas flow rate will not cause too much dynamic variation for the PCC system; and

(7) Regarding the re-boiler temperature change, the dynamic behavior variation of PCC system is limited within 383-385K and 387-388K operating regions. However, for a temperature change within 385-387K, which is the optimal range for the efficient operation of PCC system, the dynamic behavior variation is very strong.

Remark 3.1: The 5% step change of input variable is considered in this paper to ensure that the dynamic behavior obtained is the behavior of PCC system closely around the initial operating point. If a big step change is added to the input variable, the system will transit to a point far away from the initial point. It thus will not become clear, which point the dynamic response obtained belongs to and the comparison of dynamic characteristics under different working conditions will become difficult to carry out.

#### 4. Disturbance Rejection Predictive Controller Design for the Flexible Operation of the solvent-based PCC process

The slow dynamics and multi-variable coupling effect of the capture process motivate us to use MPC to enhance the flexible operation ability of the PCC system. However, in the case of wide range load change, the variation of operating conditions will change the dynamic behavior of the PCC system. The resulting modelling mismatches will degrade the performance of the linear predictive control designed for a given operating point or even cause the control system unstable.

The dynamics investigation results in Section 3 show that, under a wide range of operation, the capture system do have very strong dynamic variations. However, if the control system can maintain the re-boiler temperature tightly around 386K, which is the optimal temperature point, the dynamic variation of the PCC system will become much weaker between 50% to 90% CO<sub>2</sub> capture rates. Therefore, without the need for nonlinear controller, it is possible to design a linear predictive controller to achieve a flexible operation of the PCC system within this range.

In order to further enhance the adaptation ability of the MPC to the flue gas flow rate variation and alleviate the effect of dynamic behavior variation and unknown disturbances, a disturbance rejection predictive controller (DRPC) is proposed in this section for the PCC system operation. The DRPC is composed by an extended state observer, a steady state target calculator and a quasi-infinite horizon MPC. The schematic diagram of the proposed DRPC is illustrated in Fig. 5.

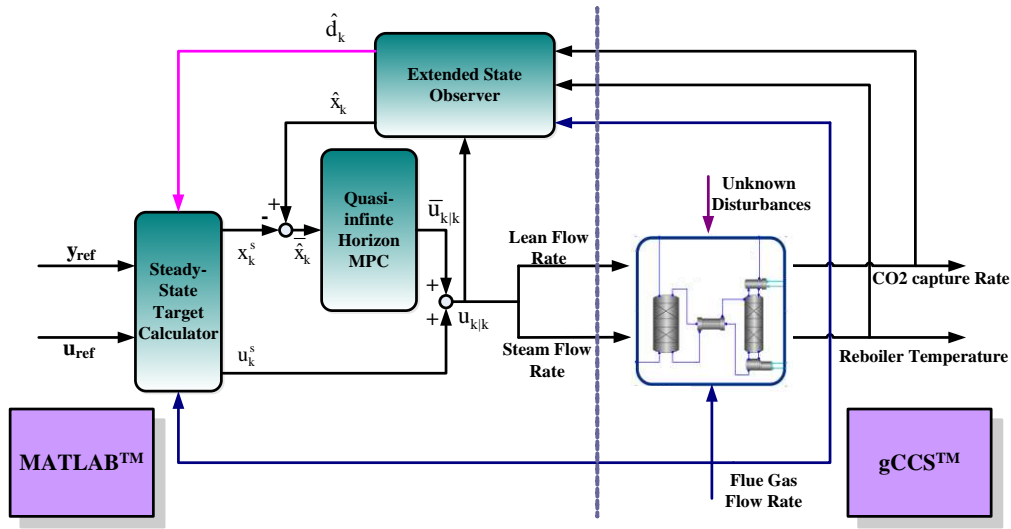


Fig. 5 Schematic diagram of the proposed DRPC for the solvent-based post combustion CO<sub>2</sub> capture system.

##### 4.1. Predictive model considering the flue gas flow rate disturbance

Considering the operating range of 50% to 90% capture rate, a linear model is identified around 70% capture rate, 386K re-boiler temperature operating point, which is the middle point within this range. To ensure the MPC can be flexibly adapted to the flue gas flow rate change, the flue gas flow rate  $f$ , which is a measured variable in power plant is taken into account as an additional input in the modeling step, resulting in the following state space model:

$$\begin{cases} x_{k+1} = Ax_k + Bu_k + Ef_k \\ y_k = Cx_k + Du_k + Ff_k \end{cases} \quad (2),$$

where  $y_k = [y_{1k} \ y_{2k}]^T$  is the output vector composed by the CO<sub>2</sub> capture rate and re-boiler temperature,  $u_k = [u_{1k} \ u_{2k}]^T$  is the input vector composed by the lean solvent flow rate  $u_1$  and re-boiler steam flow rate  $u_2$ ,  $f_k$  is the flue gas flow rate,  $x_k$  is the state vector, which do not have physical meanings; and  $A, B, C, D, E, F$  are the system matrices.

Because the flue gas flow rate is regarded as an additional input, model (2) can be rewritten into an augmented form (3):

$$\begin{cases} x_{k+1} = Ax_k + \tilde{B}\tilde{u}_k \\ y_k = Cx_k + \tilde{D}\tilde{u}_k \end{cases} \quad (3),$$

in which  $\tilde{u}_k = [u_k^T \ f_k^T]^T$  is the augmented input, and  $\tilde{B} = [B \ E]$ ,  $\tilde{D} = [D \ F]$  are the augmented system matrices. Since

394 model (3) is a standard 3-input, 2-output state space model, using the collected dynamic input, output data sequence,  
 395 conventional identification approach can be directly employed to identify the system matrices.

#### 396 4.2. Extended state observer design

397 To improve the disturbance rejection property of the MPC, i.e., to overcome the issues such as plant behavior variation and  
 398 unknown disturbances, a disturbance term  $d_k \in \mathbb{R}^2$  is introduced to the state-space model (3):

$$399 \begin{cases} x_{k+1} = Ax_k + \tilde{B}\tilde{u}_k + Gd_k \\ y_k = Cx_k + \tilde{D}\tilde{u}_k \end{cases} \quad (4).$$

400 where  $d_k$  is a lumped disturbance term representing all the effect of plant behavior variation, modeling mismatches or other  
 401 unknown disturbances. Because the state vector  $x_k$  and the disturbance term  $d_k$  are immeasurable, an extended state observer  
 402 (ESO) is designed to estimate their values:

$$403 \begin{cases} \begin{bmatrix} \hat{x}_{k+1} \\ \hat{d}_{k+1} \end{bmatrix} = \begin{bmatrix} A & G \\ 0 & I \end{bmatrix} \begin{bmatrix} \hat{x}_k \\ \hat{d}_k \end{bmatrix} + \begin{bmatrix} \tilde{B} \\ 0 \end{bmatrix} \tilde{u}_k + L[\hat{y}_k - y_k] \\ \hat{y}_k = C\hat{x}_k + \tilde{D}\tilde{u}_k \end{cases} \quad (5)$$

404 where the symbol “^” indicates the estimation. The observer gain  $L$  can be calculated by solving the following Linear  
 405 matrix inequality (LMI):

$$406 \begin{bmatrix} M_O^T + M_O - X & (M_O A^{\text{ext}} + N_O C^{\text{ext}})^T \\ M_O A^{\text{ext}} + N_O C^{\text{ext}} & X \end{bmatrix} > 0 \quad (6),$$

407 in which  $M_O$  and  $N_O$  are matrices,  $X$  is a symmetric positive definite matrix and the extended matrices  $A^{\text{ext}} = \begin{bmatrix} A & G \\ 0 & I \end{bmatrix}$ ,

408  $C^{\text{ext}} = [C \ 0]$ . The ESO gain can be determined by:  $L = M_O^{-1}N_O$  [49].

#### 409 4.3. Steady-state target calculator design

410 After the lumped disturbance signal is estimated, it will be sent to the following steady-state target calculator (SSTC) (7)-(9) to  
 411 modify the target value and control input, so that the influence of disturbances on control can be eliminated in time [50].

$$412 \min_{x_k^s, u_k^s} (u_k^s - u_{\text{ref}})^T (u_k^s - u_{\text{ref}}) \quad (7)$$

$$413 \text{ s.t. } \begin{bmatrix} x_k^s \\ y_{\text{ref}} \end{bmatrix} = \begin{bmatrix} A \\ C \end{bmatrix} x_k^s + \begin{bmatrix} \tilde{B} \\ \tilde{D} \end{bmatrix} \begin{bmatrix} u_k^s \\ f_k \end{bmatrix} + \begin{bmatrix} G \\ 0 \end{bmatrix} \hat{d}_k \quad (8)$$

$$414 u_{\min} \leq u_k^s \leq u_{\max} \quad (9)$$

415 Within the SSTC (7)-(9),  $y_{\text{ref}}$  and  $u_{\text{ref}}$  are the desired output set-points and the corresponding input values under nominal  
 416 condition;  $u_{\min}$  and  $u_{\max}$  are the constraints for the input variables. At every sampling time  $k$ , by using the static disturbance model

417 (8), the SSTC will adjust the steady state target of the state and input variables  $x_k^s, u_k^s$  according to the current flue gas flow rate

418  $f_k$  and the estimated lumped disturbance  $\hat{d}_k$ . In this way, the adverse effects of various disturbances can be quickly removed and

419 an offset-free tracking of the desired set-points  $y_{\text{ref}}$  can be achieved.

420 Considering the stability of the ESO (5), subtract (8) from (4), we can have:

$$421 \begin{cases} \bar{x}_{k+1} = A\bar{x}_k + B\bar{u}_k \\ \bar{y}_k = C\bar{x}_k + D\bar{u}_k \end{cases} \quad (10),$$

422 in which  $\bar{x}_k = x_k - x_k^s$ ,  $\bar{u}_k = u_k - u_k^s$ ,  $\bar{y}_k = y_k - y_{ref}$ . The system (10) can be used as the predictive model of the MPC, and the  
 423 goal of the control is to find the optimal constrained control sequence to drive  $\bar{y}_k$  to the zero.

#### 424 4.4. Quasi-infinite horizon MPC design

425 Considering the control objective function (11):

$$426 \quad J_0^{N_p}(k) = \sum_{N=0}^{N_p} [\bar{y}_{k+N|k}^T Q_0 \bar{y}_{k+N|k} + \bar{u}_{k+N|k}^T R_0 \bar{u}_{k+N|k}] \quad (11),$$

427 where  $\bar{y}_{k+N|k}$ , ( $N: 0 - N_p$ ) is the prediction of future output and  $\bar{u}_{k+N|k}$ , ( $N: 0 - N_p$ ) is the future control input sequence;  $Q_0$  and  
 428  $R_0$  are the weighting matrices for the output and input, respectively. A regular MPCs with enhanced disturbance rejection  
 429 property can be designed for the PCC process. At every sampling time  $k$ , through minimization of (11) subject to corresponding  
 430 input magnitude and rate constraints, the optimal future control sequence  $\bar{u}_{k+N|k}$ , ( $N: 0 - N_p$ ) can be calculated. The first  
 431 control input  $u_{k|k} = \bar{u}_{k|k} + u_k^s$  can be selected as the current control action and implemented on the PCC plant.

432 Note that the selection of this objective function requires the controller to track the desired CO<sub>2</sub> capture rate set-point rapidly  
 433 and smoothly while maintaining the re-boiler temperature closely around its optimal value to avoid the huge dynamics change of  
 434 the system. On the other hand, during the operation, the lean solvent flow rate and re-boiler steam flow rate are expected to be as  
 435 small as possible, so that better economic performance can be attained.

436 One issue for applying the regular MPCs on the PCC process is that, a large predictive horizon is usually needed to ensure a  
 437 satisfactory control quality and system stability, because the PCC process has very slow dynamics. Such a method will increase  
 438 the computational cost of the controller. To overcome this issue, a quasi-infinite horizon MPC [51] is selected in this section for  
 439 the PCC system control.

440 Consider an infinite horizon control objective function

$$441 \quad J_0^\infty(k) = \sum_{N=0}^{\infty} [\bar{y}_{k+N|k}^T Q_0 \bar{y}_{k+N|k} + \bar{u}_{k+N|k}^T R_0 \bar{u}_{k+N|k}] \quad (12),$$

442 divide the future control sequence  $\bar{u}_{k+N|k}$ , ( $N: 0 - \infty$ ) into two part: free control sequence  $\bar{U}_k = [\bar{u}_{k|k} \quad \bar{u}_{k+1|k} \quad \dots \quad \bar{u}_{k+N_f-1|k}]$   
 443 like conventional MPC for  $0 \leq N < N_f$  and feedback control sequence  $\bar{u}_{k+N|k} = YG^{-1}\bar{x}_{k+N|k}$  for  $N \geq N_f$ , in which  $Y$  and  $G$  are  
 444 matrices. By finding  $\gamma$ , the upper bound of the infinite horizon function (12), and minimizing it, the optimal control sequence can  
 445 be determined from solving the following LMIs:

$$446 \quad \begin{aligned} & \min_{\gamma, \bar{U}_k, Y, G, \tilde{s}} \gamma \\ & \text{s.t. (14) - (17)} \end{aligned} \quad (13)$$

$$447 \quad \begin{bmatrix} 1 & * & * & * & * \\ I_x \bar{x}_k + I_u \bar{U}_k & \frac{\tilde{s}}{2} & 0 & 0 & 0 \\ Q^{1/2}(L_x \bar{x}_k + L_u \bar{U}_k) & 0 & \frac{\gamma I}{2} & 0 & 0 \\ R^{1/2} \bar{U}_k & 0 & 0 & \gamma I & 0 \\ I_x w & 0 & 0 & 0 & \frac{\tilde{s}}{2} \end{bmatrix} \geq 0 \quad (14)$$

$$\begin{bmatrix} \mathbf{G} + \mathbf{G}^T - \tilde{\mathbf{S}} & * & * & * \\ (\mathbf{A}\mathbf{G} + \mathbf{B}\mathbf{Y}) & \tilde{\mathbf{S}} & \mathbf{0} & \mathbf{0} \\ \mathbf{Q}_0^{1/2}(\mathbf{C}\mathbf{G} + \mathbf{D}\mathbf{Y}) & \mathbf{0} & \gamma\mathbf{I} & \mathbf{0} \\ \mathbf{R}_0^{1/2}\mathbf{Y} & \mathbf{0} & \mathbf{0} & \gamma\mathbf{I} \end{bmatrix} > \mathbf{0} \quad (15)$$

$$\begin{bmatrix} \mathbf{I}_2 \\ \mathbf{I}_2 \\ \vdots \\ \mathbf{I}_2 \end{bmatrix} (\mathbf{u}_{\min} - \mathbf{u}_k^s) \leq \bar{\mathbf{U}}_k \leq \begin{bmatrix} \mathbf{I}_2 \\ \mathbf{I}_2 \\ \vdots \\ \mathbf{I}_2 \end{bmatrix} (\mathbf{u}_{\max} - \mathbf{u}_k^s) \quad (16)$$

$$\begin{bmatrix} \mathbf{I}_2 \\ \mathbf{I}_2 \\ \vdots \\ \mathbf{I}_2 \end{bmatrix} \Delta \mathbf{u}_{\min} \leq \zeta \left[ \bar{\mathbf{U}}_k + \begin{bmatrix} \mathbf{u}_{k-1} \\ \mathbf{I}_2 \\ \vdots \\ \mathbf{I}_2 \end{bmatrix} \mathbf{u}_k^s \right] \leq \begin{bmatrix} \mathbf{I}_2 \\ \mathbf{I}_2 \\ \vdots \\ \mathbf{I}_2 \end{bmatrix} \Delta \mathbf{u}_{\max} \quad (17)$$

where  $\mathbf{Q} = \mathbf{I}_{N_f} \otimes \mathbf{Q}_0$ ,  $\mathbf{R} = \mathbf{I}_{N_f} \otimes \mathbf{R}_0$ ,  $w$  is the upper bound of the state estimation error,  $\bar{\hat{\mathbf{x}}}_k = \hat{\mathbf{x}}_k - \mathbf{x}_k^s$  and

$$\zeta = \begin{bmatrix} -\mathbf{I}_2 & \mathbf{I}_2 & \mathbf{0} & \dots & \mathbf{0} \\ \mathbf{0} & -\mathbf{I}_2 & \mathbf{I}_2 & \dots & \vdots \\ \vdots & \vdots & \ddots & \ddots & \mathbf{0} \\ \mathbf{0} & \dots & \mathbf{0} & -\mathbf{I}_2 & \mathbf{I}_2 \end{bmatrix}. \text{ The prediction matrices } \mathbf{l}_x, \mathbf{l}_u, \mathbf{L}_x, \mathbf{L}_u \text{ can be obtained by stacking up the predictive model}$$

(10):

$$\mathbf{l}_x = \mathbf{A}^{N_f}, \mathbf{l}_u = \begin{bmatrix} \mathbf{A}^{N_f-1} & \mathbf{A}^{N_f-2} & \dots & \mathbf{A}^0 \end{bmatrix} \mathbf{B},$$

$$\mathbf{L}_x = \begin{bmatrix} \mathbf{C} \\ \mathbf{C}\mathbf{A} \\ \vdots \\ \mathbf{C}\mathbf{A}^{N_f-1} \end{bmatrix}, \mathbf{L}_u = \begin{bmatrix} \mathbf{D} & \mathbf{0} & \dots & \mathbf{0} \\ \mathbf{C}\mathbf{B} & \mathbf{D} & \dots & \mathbf{0} \\ \vdots & \ddots & \dots & \mathbf{0} \\ \mathbf{C}\mathbf{A}^{N_f-2}\mathbf{B} & \dots & \mathbf{C}\mathbf{B} & \mathbf{D} \end{bmatrix}.$$

The LMI (14) guarantees that,  $\gamma$  is the upper bound of the infinite objective function (12), (15) gives the Lyapunov stability constraint of the closed loop control system, (16) and (17) are the magnitude and rate constraints of the free input variables. At each sampling time, the first element in the solved control sequence  $\bar{\mathbf{u}}_{k|k}$  is added to the target input  $\mathbf{u}_k^s$ , the resulting  $\mathbf{u}_{k|k} = \bar{\mathbf{u}}_{k|k} + \mathbf{u}_k^s$  is selected as the current control action and implemented on the PCC plant.

The proposed DRPC has the following advantages for the flexible operation of the PCC process:

1) Flue gas flow rate variation of upstream power plant is a major disturbance to the PCC process. To overcome this issue, the flue gas flow rate is used as an additional input in the model development based on the idea of feed-forward control. Then by using the ESO and SSTC, the proposed DRPC can change the target input  $\mathbf{u}_k^s$  immediately according to the current flue gas flow rate, thus the control action  $\mathbf{u}_{k|k} = \bar{\mathbf{u}}_{k|k} + \mathbf{u}_k^s$  can be promptly adjusted, making the capture system flexibly adapt to the flue gas flow rate change;

2) Plant dynamic variations due to wide range of operation and other unknown disturbances will bring in many adverse

467 effects to the control of PCC process. For this reason, the ESO and SSTC are designed in the DRPC structure to estimate  
468 the disturbances and eliminate their impact, enhance the disturbance rejection property of the MPC; and

469 3) A quasi-infinite horizon MPC is applied for the PCC process. By including the infinite future control moves into a  
470 feedback control law, only a fewer prediction steps are required to achieve a satisfactory control of the slow PCC process.

471 Remark 4.1: For the initialization of the MPC, we assume that the PCC system is in steady state at the initial moment  
472 and there are no lumped disturbances ( $\hat{d}_k=0$ ). Then according to the current input  $u_k$ , output  $y_k$  ( $y_k=y_{ref}$ ,  $u_k=u_{ref}$ ) and flue  
473 gas flow rate  $f_k$ ,  $x_k^s$  can be calculated by equation (7)-(9), which is set as the initial state  $\hat{x}_k$ .

## 474 5. Simulation Results

475 This section verifies the control effect of DRPC for the flexible operation of the PCC process under wide range CO<sub>2</sub>  
476 capture rate change, flue gas flow rate change and unknown disturbances. Linear state space model identified around 70%  
477 capture rate, 386K operating point for re-boiler temperature is selected as the predictive model, since it is a middle point  
478 within the considered operating range (50%-90% capture rates). The parameters of the proposed DRPC are set as follows:  
479 sampling time  $T_s=30s$ , free control input number  $N_f=2$ , disturbance matrix  $G=\text{diag}(0.1, 0.08)$ , upper bound of the state  
480 estimation error  $w=[1 \ 1]^T$ . A too small  $w$  will limit the feasibility of the DRPC; and a too large  $w$  will influence the  
481 initial status of the predictive control system. Considering the objectives of the PCC system control:1) quickly track the  
482 CO<sub>2</sub> capture rate set-point; 2) maintain the re-boiler temperature at optimal point to avoid plant behavior variation; and 3)  
483 reduce the lean solvent and re-boiler steam flow rate as much as possible to lower the energy consumption, the weighting  
484 matrices are set as  $Q_0=\text{diag}(10, 1)$ ,  $R_0=\text{diag}(1, 1)$ . Input magnitude and rate constraints are taken into  
485 account:  $u_{\min}=[0.2 \ 0.005]^T$ ,  $u_{\max}=[1 \ 0.08]^T$ ;  $\Delta u_{\min}=[-0.007 \ -0.001]^T$ ,  $\Delta u_{\max}=[0.007 \ 0.001]^T$  due to the physical  
486 limitations of the valves and pumps.

487 Two other MPCs are designed for the purpose of comparison: a) the conventional MPC with integral action (MPC\_I); b)  
488 conventional MPC without using the integral action (MPC). The predictive model, sampling time and weighting matrices  
489 of these two MPCs are set the same as the DRPC. The prediction horizon  $N_p$  is set as 6 steps (180s) because too small  $N_p$  is  
490 very easy to cause system instability.

491 The three predictive controllers are developed in MATLAB platform and run with a sample period of 30s. At each  
492 sampling time during the simulation, the controllers and the gCCS plant model communicated with each other through the  
493 gO:MATLAB interface.

494 Case 1: Wide range CO<sub>2</sub> capture rate change is considered in the first simulation since it is a basic requirement for the  
495 flexible operation of the PCC process. We suppose that the PCC system is operating at 70% capture rate point initially,  
496 then according to the instruction of scheduling level, at  $t=10\text{min}$  and  $t=160\text{min}$ , the set-point changes to 50% and 90%  
497 at the ramping rate of 0.4%/min respectively. During the CO<sub>2</sub> capture rate variation, the set-point of re-boiler temperature  
498 controller is fixed at 386K.

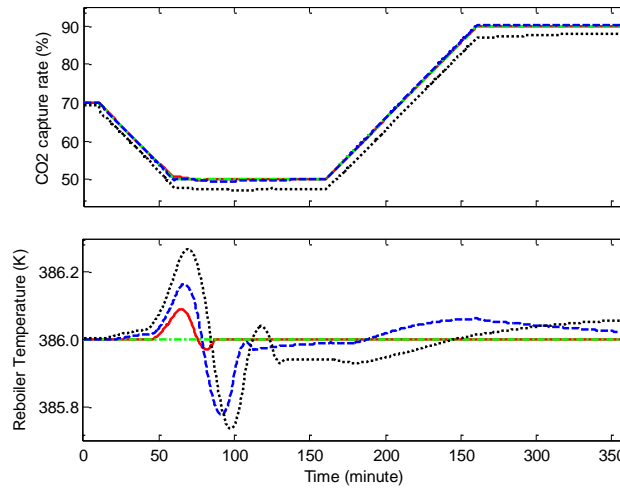


Fig. 6. Performance of the PCC system for a 70%-50%-90% CO<sub>2</sub> capture rate change: output variables (solid in red: DRPC; dashed in blue: MPC\_I; dotted in black: MPC; dot-dashed in green: reference).

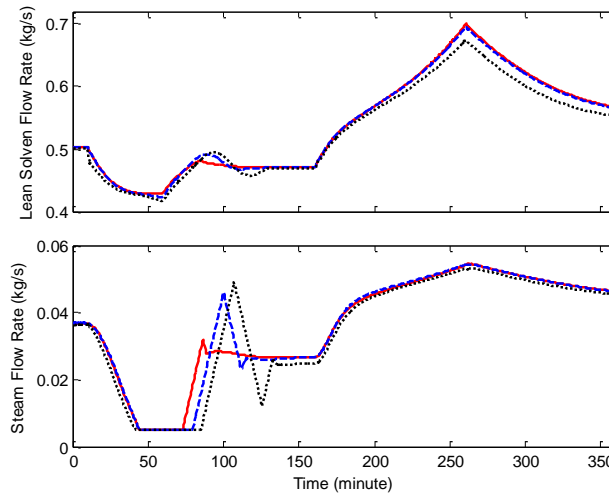


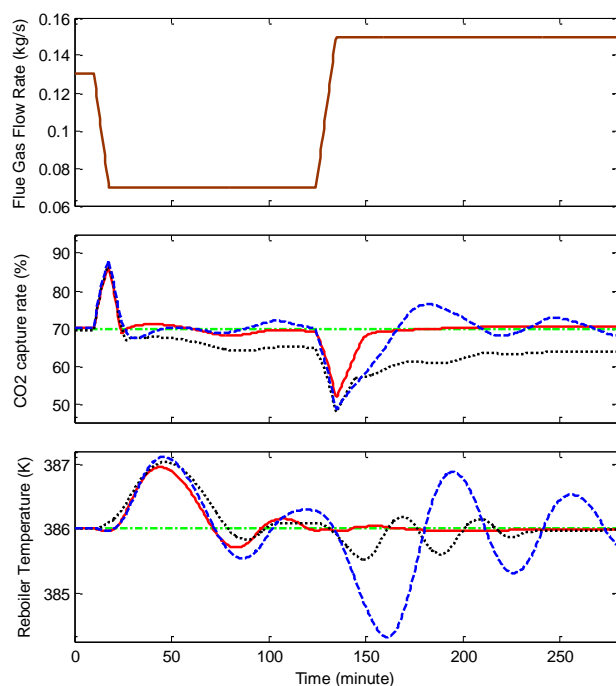
Fig. 7. Performance of the PCC system for a 70%-50%-90% CO<sub>2</sub> capture rate change: manipulated variables (solid in red: DRPC; dashed in blue: MPC\_I; dotted in black: MPC)

The results in Figs. 6 and 7 indicate that all the three linear predictive controllers can attain a satisfactory control performance for the CO<sub>2</sub> capture rate change within 50%-90% operating region. When the capture rate set-point varies, the predictive controllers adjust the lean solvent and re-boiler steam flow rates coordinately, the CO<sub>2</sub> capture rate can thus follow the changed set-point closely and smoothly. At the same time, the re-boiler temperature can also be kept tightly around the desired point, ensuring an economical running of the PCC process and avoiding the adverse impact of strong dynamic changes on the control system.

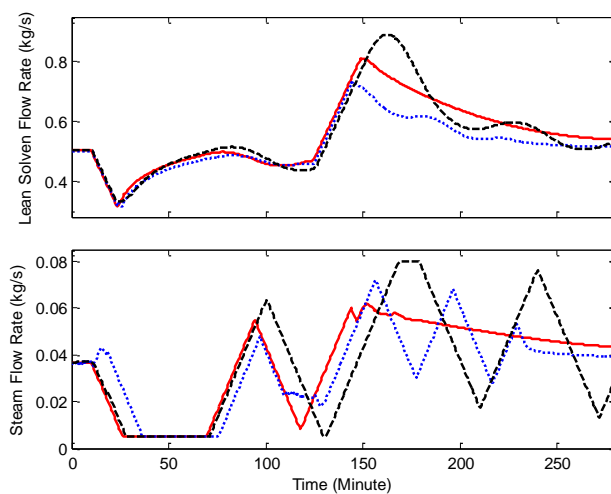
By using the ESO and SSTC to estimate and quickly compensate the effect of dynamic variation during the capture rate change, the proposed DRPC has the best performance among the three linear predictive controllers. The deviation of the re-boiler temperature is less than 0.1K and the steam flow rate fluctuation during the transition of regulation is quite small. Note that with the use of quasi-infinite horizon MPC in the DRPC framework, the free control input number is set quite small as  $N_f=2$ , which means that the computational effort for the DRPC could be very small. With the integral action being included in the MPC design, an offset free tracking performance can also be achieved by the MPC\_I, however, in the case of small predictive horizon, the performance of MPC\_I is worse than the DRPC, which is mainly reflected in the re-boiler temperature control. For the conventional MPC, since no means are used to compensate for the effects of dynamic change, it has the worst performance. Control offset is occurred for both the CO<sub>2</sub> capture rate and re-boiler temperature.

Case 2: Flue gas flow rate change is then considered in the second simulation to test the performance of the linear MPCs. We assume that at  $t=10\text{min}$  and  $t=125\text{min}$ , due to the power load variation of upstream power plant, the flue gas flow rate

522 changes from 0.13kg/s to 0.07kg/s and 0.15kg/s respectively. During the simulation, the set-points for CO<sub>2</sub> capture rate and  
523 re-boiler temperature are fixed at 70% and 386K. The results are illustrated in Figs. 8 and 9.



524  
525 Fig. 8. Performance of the PCC system in the presence of power plant flue gas variation: output variables (solid in red: DRPC; dashed in blue: MPC\_I; dotted  
526 in black: MPC; dot-dashed in green: reference).



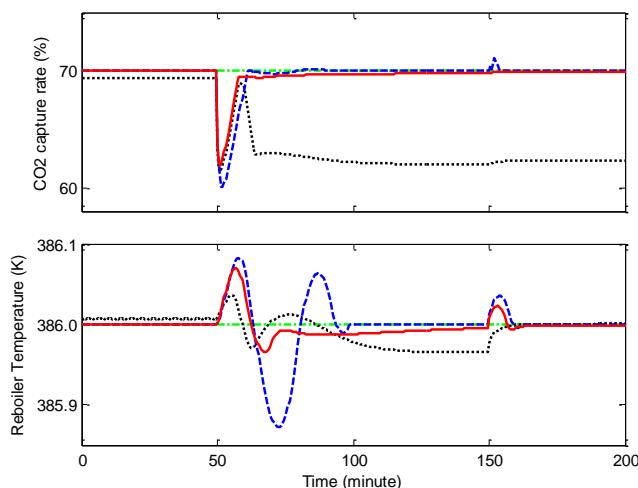
527  
528 Fig. 9. Performance of the PCC system in the presence of power plant flue gas variation: manipulated variables (solid in red: DRPC; dashed in blue: MPC\_I;  
529 dotted in black: MPC)

530 The simulation results demonstrate that the proposed DRPC can effectively handle the variation of flue gas flow rate. As  
531 shown in Figs. 2-4, the dramatic change of the flue gas flow rate will cause large changes in CO<sub>2</sub> capture rate rapidly and  
532 make it deviate far away from the desired set-point under open loop situation. However, because the flue gas flow rate  $f$   
533 has already been considered in the predictive model development, through the calculation of SSTC, the DRPC can regulate  
534 the lean solvent and re-boiler steam flow rate in time, according to the current flue gas flow rate. As a result, it can be seen  
535 in Fig. 8 that, the capture rate can be quickly controlled back to the set-point and the fluctuation of re-boiler temperature  
536 during the regulation is greatly reduced.

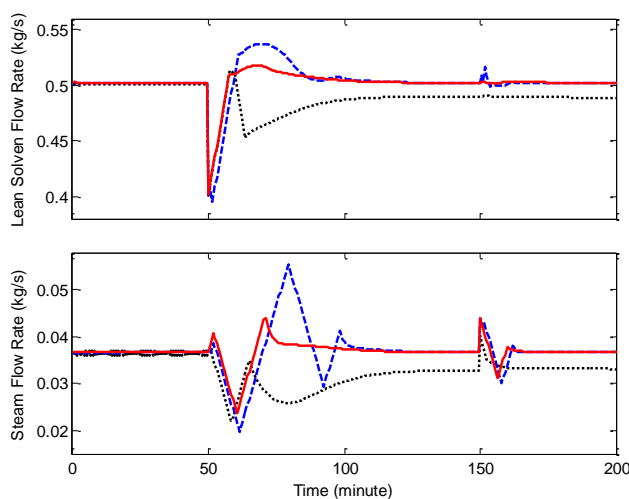
537 For the other two MPCs, their performance is much worse than the proposed DRPC. In the presence of flue gas flow  
538 rate variation, their prediction and control performance is greatly degraded since the flue gas is not considered in the model  
539 development. Regarding the conventional MPC, large control offset is occurred for the CO<sub>2</sub> capture rate, and the re-boiler

540 temperature has continued to swing around the given set-point. Meanwhile, the lean solvent and steam flow rates also  
 541 exhibit a greater degree of oscillation compared with the performance of DRPC. Regarding the MPC\_I, the use of integral  
 542 action reduces the stability of the control system. Severe fluctuation can be viewed for both the capture rate and re-boiler  
 543 temperature in Fig. 8 and for steam flow rate in Fig. 9. The PCC system is not able to run smoothly under the strong  
 544 variation of flue gas flow rate.

545 Case 3: We then devise the last simulation to test the performance of the linear predictive controllers in the presence of  
 546 unknown disturbances. Similarly, we suppose that the PCC plant is operating at 70% capture rate operating point initially,  
 547 due to some unknown equipment failures, at  $t=50\text{min}$ , the lean solvent flow rate is reduced by  $0.1\text{kg/s}$ , then at  $t=150\text{min}$ ,  
 548 the re-boiler steam flow rate is increased by  $0.0074\text{kg/s}$ . The set-points for  $\text{CO}_2$  capture rate and re-boiler temperature are  
 549 fixed at 70% and  $386\text{K}$  during the simulation.



550  
 551 Fig. 10. Performance of the PCC system in the presence of unknown disturbances: output variables (solid in red: DRPC; dashed in blue: MPC\_I; dotted in  
 552 black: MPC; dot-dashed in green: reference ).



553  
 554 Fig. 11. Performance of the PCC system in the presence of unknown disturbances: manipulated variables (solid in red: DRPC; dashed in blue: MPC\_I; dotted  
 555 in black: MPC).

556  
 557 The simulation results shown in Figs. 10 and 11 illustrate the effectiveness of the proposed DRPC in handling the impact  
 558 of unknown disturbances. At  $t=50\text{ min}$ , the unknown decrease of lean solvent flow rate makes the  $\text{CO}_2$  capture rate and  
 559 re-boiler temperature increase rapidly. The DRPC estimates the value of disturbance  $\hat{d}_k$  from the control action and  
 560 actual plant output via the ESO, then quickly modifies the lean solvent and steam flow rates according to the value of  $\hat{d}_k$

561 through the SSTC. Following this, the impact of unknown disturbances can be rapidly rejected by the DRPC system. The  
562 same situation also occurs at  $t=150$  min, when unknown increase of steam flow rate make the  $\text{CO}_2$  capture rate and  
563 re-boiler temperature rise. The DRPC can drive them back to the set-points with minimal fluctuations and time. On the  
564 other hand, by including the integral action, the MPC\_I can also alleviate the influence of unknown disturbances, however,  
565 its performance is worse than the DRPC, stronger fluctuation can be viewed from the re-boiler temperature control. For the  
566 conventional MPC, the influence of unknown disturbances cannot be eliminated, large control offset is thus occurred,  
567 especially for the  $\text{CO}_2$  capture rate.

568 The three simulations demonstrate the advantages of the proposed DRPC in the operation of the PCC process. The  
569 DRPC can quickly change the  $\text{CO}_2$  capture rate in a wide range, respond flexibly to the flue gas flow rate variation and  
570 effectively overcome the impact of unknown disturbances.

## 571 **6. Conclusion**

572 This paper investigated the dynamic behavior and its variation of the PCC system to provide guidance for the controller design.  
573 The variation of three key variables during the PCC flexible operation are taken into account: the  $\text{CO}_2$  capture rate, the power  
574 plant flue gas flow rate and the re-boiler temperature. Step response tests at different operating points are performed to display  
575 the dynamic characteristics of the PCC system intuitively.

576 The investigation results fully illustrate the slow dynamics of the PCC system and the strong couplings among the key  
577 variables. The dynamic behavior variation of the PCC system is also exhibited, that: 1) under higher capture rate and flue gas  
578 flow rate, the responses of PCC system is quicker compared with lower conditions 2) there are two regions within which the  
579 dynamic variation of the PCC system is quite strong: around 90%-95% capture rate range and around 386K, the optimal re-boiler  
580 temperature point.

581 To overcome the control difficulties of the PCC system and enhance the performance of conventional MPC in the presence of  
582 dynamic variations, a disturbance rejection predictive controller (DRPC) is developed for the PCC process. By considering the  
583 effects of flue gas flow rate in the predictive model development and coordinated using the extended state observer (ESO),  
584 steady state target calculator (SSTC) and a quasi-infinite horizon MPC. The DRPC can quickly adapt to the flue gas flow rate  
585 change, eliminate the effect of plant behavior variation and unknown disturbances and achieve a wide range of capture rate  
586 change using very small prediction steps. Simulation results on an MEA based PCC plant verify the advantages and  
587 effectiveness of the proposed DRPC.

## 588 **Acknowledgements**

589 The authors would like to acknowledge the National Natural Science Foundation of China (NSFC) under Grant 51506029, the  
590 Natural Science Foundation of Jiangsu Province, China under Grant BK20150631, China Postdoctoral Science Foundation, EU  
591 FP7 International Staff Research Exchange Scheme on power plant and carbon capture (Ref: PIRSES-GA-2013-612230) for  
592 funding this work.

## 593 **References**

- 594 [1] IPCC. Special report on carbon dioxide capture and storage. Cambridge, UK: Cambridge University Press, 2005.
- 595 [2] IPCC. Climate change 2007: synthesis report. Contribution of working groups I, II and III to the fourth assessment report of the intergovernmental panel on  
596 climate change (pp. 30–37). Geneva, Switzerland, 2007.
- 597 [3] IEA. Energy Technology Perspectives 2008. IEA/OECD, Paris, France, 2008.
- 598 [4] J. Oexmann. Post-Combustion  $\text{CO}_2$  Capture: Energetic Evaluation of chemical Absorption Processes in Coal-Fired Steam Power Plants. Ph.D. thesis,  
599 Technische Universitat Hamburg-Harburg, 2011.
- 600 [5] J. Oexmann, C. Hensel and A. Kather. Post-combustion  $\text{CO}_2$ -capture from coal-fired power plants: preliminary evaluation of an integrated chemical  
601 absorption process with piperazine-promoted potassium carbonate. International Journal of Greenhouse Gas Control, vol. 2, pp. 539–552, 2008.
- 602 [6] P. Mores, N. Rodríguez, N. Scenna and S. Mussati.  $\text{CO}_2$  capture in power plants: Minimization of the investment and operating cost of the post-combustion  
603 process using MEA aqueous solution. International Journal of Greenhouse Gas Control, vol. 10, pp. 148–163, 2012.

- 604 [7] A. Raksajati, M. T. Ho and D. E. Wiley. Reducing the cost of CO<sub>2</sub> capture from flue gases using aqueous chemical absorption. *Ind. Eng. Chem. Res.*, vol. 52,  
605 no. 47, pp. 16887-16901, Nov 2013.
- 606 [8] M. Karimi, H. F. Svendsen and M. Hillestad. Capital costs and energy considerations of different alternative stripper configurations for post combustion  
607 CO<sub>2</sub> capture. *Chemical Engineering Research and Design*, vol. 89, no. 8, pp. 1229–1236, 2011.
- 608 [9] L. Duan, M. Zhao and Y. Yang. Integration and optimization study on the coal-fired power plant with CO<sub>2</sub> capture using MEA. *Energy*, vol. 45, pp.107-116,  
609 2012.
- 610 [10] Q. Chen, C. Kang, Q. Xia and D. S. Kirschen. Optimal flexible operation of a CO<sub>2</sub> capture power plant in a combined energy and carbon emission market.  
611 *IEEE Trans. Power Syst.*, vol. 27, no. 3, pp.1602-1608, Aug. 2012.
- 612 [11] A. Lawal, M. Wang, P. Stephenson and O. Obi. Demonstrating full-scale post-combustion CO<sub>2</sub> capture for coal-fired power plants through dynamic  
613 modelling and simulation. *Fuel*, vol. 101, pp. 115-128, 2012.
- 614 [12] A. Lawal, M. Wang, P. Stephenson, G. Koumpouras and H. Yeung. Dynamic modelling and analysis of post-combustion CO<sub>2</sub> chemical absorption process  
615 for coal-fired power plants. *Fuel*, vol. 89, pp. 2791-2801, 2010.
- 616 [13] A. Arce, N. Mac Dowell, N. Shah and L.F. Vega. Flexible operation of solvent regeneration systems for CO<sub>2</sub> capture processes using advanced control  
617 techniques: Towards operational cost minimization. *International Journal of Greenhouse Gas Control*, vol. 11, pp. 236-250, 2012.
- 618 [14] N. A. Manaf, A. Qadir and A. Abbas. The hybrid MPC-MINLP algorithm for optimal operation of coal-fired power plants with solvent based  
619 post-combustion CO<sub>2</sub> capture. *Petroleum*, vol. 3, pp. 155-166, 2017.
- 620 [15] Y. Lin, T. Pan, D. Wong, S. Jang, Y. Chi and C. Yeh. Plantwide control of CO<sub>2</sub> capture by absorption and stripping using monoethanolamine solution. *Ind*  
621 *Eng Chem Res*, vol. 50, pp. 1338-1345, 2011.
- 622 [16] Y. Lin, D. Wong and S. Jang. Control strategies for flexible operation of power plant with CO<sub>2</sub> capture plant. *AIChE Journal*, vol. 58, no. 9, pp. 2697-2704,  
623 2012.
- 624 [17] A. Cormos, M. Vasile and M. Cristea. Flexible operation of CO<sub>2</sub> capture processes integrated with power plant using advanced control techniques. 12th  
625 International Symposium on Process Systems Engineering and 25th European Symposium on Computer Aided Process Engineering, Copenhagen, Denmark,  
626 May 31-Jun 4, 2015.
- 627 [18] Z. He, M. H. Sahraei, and L. A. Recardez-Sandoval. Flexible operation and simultaneous scheduling and control of a CO<sub>2</sub> capture plant using model  
628 predictive control. *International Journal of Greenhouse Gas Control*, vol. 48, pp. 300-311, 2016.
- 629 [19] M. Bui, I. Gunawan, V. Verheyen, P. Feron and E. Meuleman. Flexible operation of CSIRO's post-combustion CO<sub>2</sub> capture pilot plant at the AGL Loy Yang  
630 power station. *International Journal of Greenhouse Gas Control*, vol. 48, pp. 188-203, 2016.
- 631 [20] M. Zaman, H. Jang, M. Rizman and J. H. Lee. Optimal design for flexible operation of the post-combustion CO<sub>2</sub> capture plant with uncertain economic  
632 factors. *Computers and Chemical Engineering*, vol. 84, pp. 199-207, 2016.
- 633 [21] X. Wu, J. Shen, Y. Li, and K. Y. Lee. Steam power plant configuration, design and control. *WIREs Energy Environ.* vol. 4, no. 6, pp. 537-563, Nov-Dec.  
634 2015.
- 635 [22] A. Lawal, M. Wang, P. Stephenson and H. Yeung. Dynamic modelling of CO<sub>2</sub> absorption for post combustion capture in coal-fired power plants. *Fuel*, vol.  
636 88, pp. 2455-2462, 2009.
- 637 [23] S. Ziaii, G.T. Rochelle and T. F. Edgar. Dynamic modeling to minimize energy use for CO<sub>2</sub> capture in power plants by aqueous monoethanolamine. *Ind. Eng.*  
638 *Chem. Res.*, vol. 48, no. 13, pp. 6105-6111, 2009.
- 639 [24] K. Dietl, A. Joos and G. Schmitz, Dynamic analysis of the absorption/desorption loop of a carbon capture plant using an object-oriented approach. *Chemical*  
640 *Engineering and Processing: Process Intensification*, vol. 52, pp.132-139, 2012.
- 641 [25] R. M. Montañés and L. O. Nord, Dynamic Simulations of the Post-combustion CO<sub>2</sub> Capture System of a Combined Cycle Power Plant. 12th International  
642 Modelica Conference, Prague, Czech Republic, May 15-17, 2017.
- 643 [26] S. A. Jayarathna, B. Lie, M. C. Melaaen, Amine based CO<sub>2</sub> capture plant: dynamic modeling and simulations. *International Journal of Greenhouse Gas*  
644 *Control*, vol. 14, pp. 282-290. 2013.
- 645 [27] J. Rodriguez, A. Andrade, A. Lawal, N. Samsatli, S. Calado, T. Lafitte, J. Fuentes and C. Pantelides. An integrated framework for the dynamic modelling of  
646 solvent-based CO<sub>2</sub> capture processes. *Energy Procedia* vol.63, pp. 1206-1217, 2014.
- 647 [28] E. Mechleri, A. Lawal, A. Ramos, J. Davison and N. M. Dowell. Process control strategies for flexible operation of post-combustion CO<sub>2</sub> capture plants.  
648 *International Journal of Greenhouse Gas Control*, vol. 57, pp. 14-25, 2017.
- 649 [29] F. Li, J. Zhang, E. Oko and M. Wang. Modelling of a post-combustion CO<sub>2</sub> capture process using neural networks. *Fuel*, vol. 151, pp. 156-163, 2015.

- 650 [30] N. A. Manaf, A. Cousins, P. Feron and A. Abbas. Dynamic modelling. Identification and preliminary control analysis of an amine-based post-combustion  
651 CO<sub>2</sub> capture pilot plant. *Journal of Cleaner Production*, vol. 113, pp. 635-653, 2016.
- 652 [31] Q. Zhou, C. W. Chan, P. Tontiwachwuthikul, R. Idem and D. Gelowitz. Application of neuro-fuzzy technique for operational problem solving in a CO<sub>2</sub>  
653 capture process system. *Journal of Greenhouse Gas Control*, vol. 15, pp. 32-41. 2013.
- 654 [32] R. Faber, M. Kopcke, O. Biede, J. N. Knudsen and J. Andersen. Open-loop responses for the MEA post combustion capture process: Experimental results  
655 from the Esbjerg pilot plant. *Energy Procedia*, vol. 4, pp. 1427-1434, 2011.
- 656 [33] M. Panahi, S. Skogestad. Economically efficient operation of CO<sub>2</sub> capturing process part I: self-optimizing procedure for selecting the best controlled  
657 variables. *Chemical Engineering and Processing: Process Intensification*, vol. 50, no.3, pp. 247-253, 2011.
- 658 [34] M. Panahi and S. Skogestad, Economically efficient operation of CO<sub>2</sub> capturing process part II: Design of control layer. *Chemical Engineering and*  
659 *Processing: Process Intensification*, vol. 52, pp. 112-124, 2012.
- 660 [35] Q. Zhang, R. Turton and D. Bhattacharyya. Development of model and model-predictive control of an MEA-based post-combustion CO<sub>2</sub> capture process.  
661 *Industrial & Engineering Chemistry Research*, vol. 55, pp. 1292-1308, 2016.
- 662 [36] T. Nittaya, P. L. Douglas, E. Croiset and L. A. Ricardez-Sandoval. Dynamic modelling and control of MEA absorption processes for CO<sub>2</sub> capture from  
663 power plants. *Fuel*, vol. 116, pp. 672-691, 2014.
- 664 [37] T. Nittaya, P. L. Douglas, E. Croiset and L. A. Ricardez-Sandoval. Dynamic Modeling and Evaluation of an Industrial-Scale CO<sub>2</sub> Capture Plant Using  
665 Monoethanolamine Absorption Processes. *Industrial & Engineering Chemistry Research*, vol. 53, pp. 11411-11426, 2014.
- 666 [38] S. Posch and M. Haider. Dynamic modelling of CO<sub>2</sub> absorption from coal-fired power plants into an aqueous monoethanolamine solution. *Chem Eng Res*  
667 *Des*, vol. 91, pp. 977-987, 2013.
- 668 [39] A. Bedelbayev, T. Greer and B. Lie. Model based control of absorption tower for CO<sub>2</sub> capturing. 49th Scandinavian Conference on Simulation and  
669 Modeling, Oct 2008.
- 670 [40] E. D. Mehleri, N. Mac Dowell and N. F. Thornhill, Model predictive control of post-combustion CO<sub>2</sub> capture process integrated with a power plant. 12th  
671 International Symposium on Process Systems Engineering and 25th European Symposium on Computer Aided Process Engineering, Copenhagen, Denmark,  
672 May 31-Jun 4, 2015.
- 673 [41] J. Åkesson, C.D. Laird, G. Lavedan, K. Pröhl, H. Tummescheit, S. Velut and Y. Zhu. Nonlinear Model Predictive Control of a CO<sub>2</sub> Post-Combustion  
674 Absorption Unit. *Chemical Engineering & Technology*, vol. 35, no. 3, pp. 445-454, 2012.
- 675 [42] K. Pröhl, H. Tummescheit, S. Velut and J. Åkesson. Dynamic model of a post-combustion absorption unit for use in a non-linear model predictive control  
676 scheme. *Energy Procedia*, vol. 4, 2620-2627, 2011.
- 677 [43] Q. Zhang, R. Turton and D. Bhattacharyya. Nonlinear model predictive control and H<sub>∞</sub> robust control for a post-combustion CO<sub>2</sub> capture process.  
678 *International Journal of Greenhouse Gas Control*, vol. 70, pp. 105-116, 2018.
- 679 [44] M. H. Sahraei and L. A. Ricardez-Sandoval. Controllability and optimal scheduling of a CO<sub>2</sub> capture plant using model predictive control. *International*  
680 *Journal of Greenhouse Gas Control*, vol. 30, pp. 58-71, 2014.
- 681 [45] M. T. Luu, N. A. Manaf and A. Abbas. Dynamic modelling and control strategies for flexible operation of amine-based post-combustion CO<sub>2</sub> capture  
682 systems. *International Journal of Greenhouse Gas Control*, vol. 39, pp. 377-389, 2015.
- 683 [46] A. Cormos, M. Vasile and M. Cristea. Flexible operation of CO<sub>2</sub> capture processes integrated with power plant using advanced control techniques. 12th  
684 International Symposium on Process Systems Engineering and 25th European Symposium on Computer Aided Process Engineering, Copenhagen, Denmark,  
685 May 31-Jun 4, 2015.
- 686 [47] X. Wu, J. Shen, Y. Li, M. Wang and A. Lawal, Flexible operation of post-combustion solvent-based carbon capture for coal-fired power plants using  
687 multi-model predictive control: a simulation study. *Fuel*, vol. 220, pp.931-941, 2018.
- 688 [48] X. Wu, J. Shen, Y. Li, M. Wang and A. Lawal, Nonlinear dynamic analysis and control design of a solvent-based post-combustion CO<sub>2</sub> capture process.  
689 *Computers & Chemical Engineering*, vol. 115, pp. 397-406, 2018.
- 690 [49] G. Feng. A survey on analysis and design of model-based fuzzy control systems. *IEEE Transactions on Fuzzy Systems*, vol. 14, no. 5, pp. 676-697, 2006.
- 691 [50] K. R. Muske and T. A. Badgwell. Disturbance modeling for offset-free linear model predictive control. *Journal of Process Control*, vol. 12, No. 5, pp.  
692 617-632, 2002.
- 693 [51] X. Wu, J. Shen, Y. Li, and K. Y. Lee. Fuzzy Modeling and Stable Model Predictive Tracking Control of Large-scale Power Plants. *Journal of Process*  
694 *Control*, vol. 24, No.10, pp. 1609-1626, 2014.
- 695